DiFranco and Vergara, http://www.jgp.org/cgi/content/full/jgp.201110682/DC1

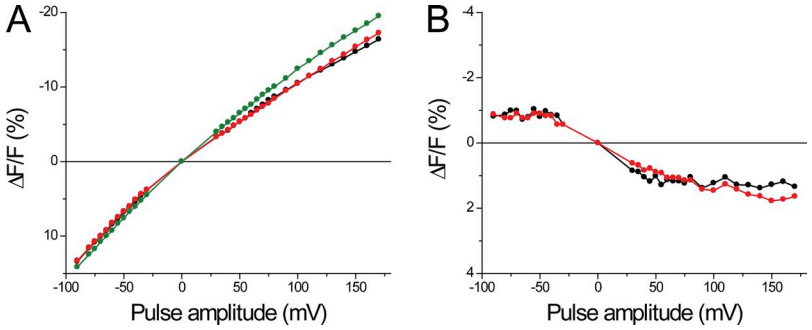

Figure S1. Voltage dependence of the steady-state and undershoot ΔF/F in di-8-ANEPPS transients detected in 1/2Na and TEA-Cl external solutions. (A) Steady-state ΔF/F values of di-8-ANEPPS transients (averaged during the period illustrated in red boxes in Fig. 3, A–F) are shown with the following symbols for different solutions: 1/2Na, black circles and lines; 1/2Na + TTX, red circles and lines; TEA-Cl +TTX, green circles and lines. Data are from the same fiber as in Fig. 3. (B) Undershoot ΔF/F values of di-8-ANEPPS transients are shown with the following symbols for different solutions: 1/2Na, black circles and lines; 1/2Na + TTX, red circles and lines.

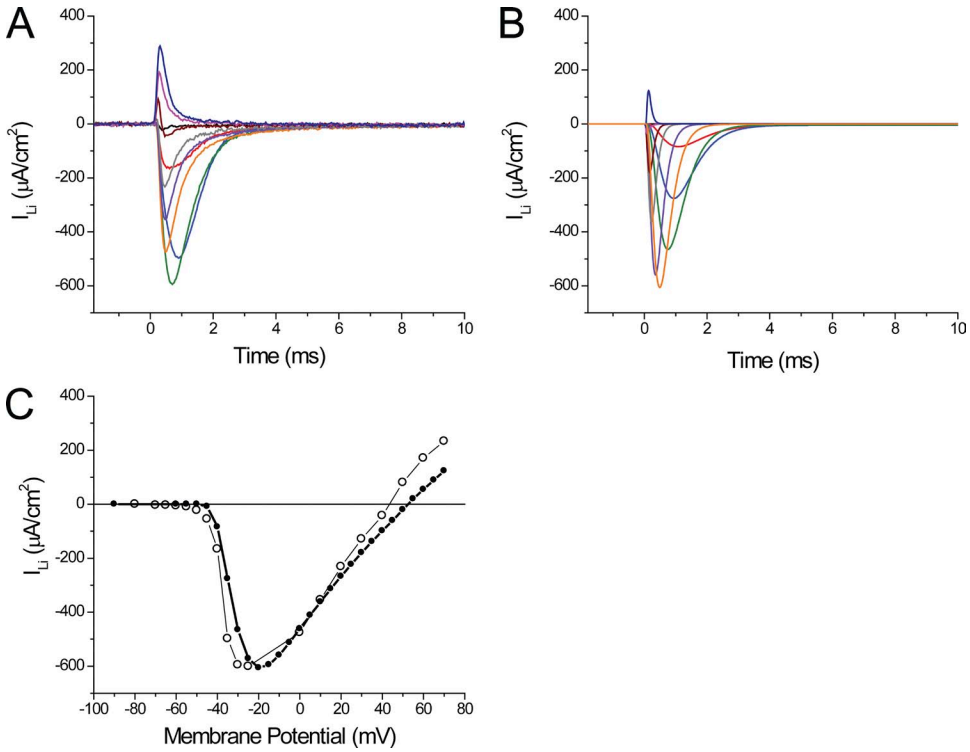

Figure S2. Model predictions of ionic currents in a detubulated fiber. (A) Lithium current traces from Fig. 7 A. (B) Model prediction of ILi. The kinetic parameters for the Na currents in this simulation were those in the Appendix. $\overline{P_{Na}} = 9.0 \times 10^{-4}$ cm/s. The values used were (C) voltage dependence of experimental (open circles) and simulated (filled circles) peak ILi, measured from data in A and B, respectively.

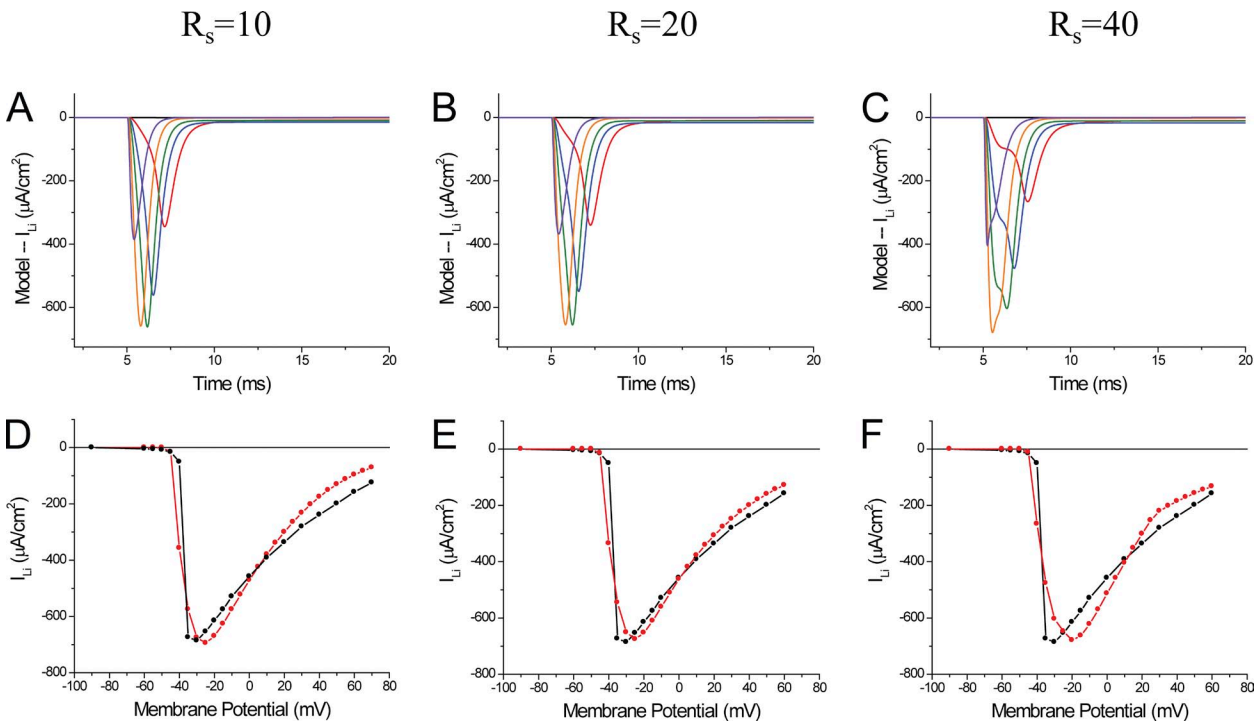

Figure S3. Effect of R_s on model predictions of I_{Li} and the voltage dependence of the overshoot and peak ILi. (A–C) Model predictions of I_{Li} in response to 40-, 50-, 55-, 60-, 70-, and 100-mV depolarizing pulses (black, red, blue, green, orange, and purple traces, respectively). The access resistance (R_s) was 10, 20, and 40 Ωcm2 for A–C, respectively. The Na channel permeability densities ($\overline{P_{Na}}$ -TTS and $\overline{P_{Na}}$ -S, respectively) were: 5.64×10^{-4} cm/s and 3.76×10^{-4} cm/s (A); 5.65×10^{-4} cm/s and 5.65×10^{-4} cm/s (B); and 5.12×10^{-4} cm/s and 10.9×10^{-4} cm/s (C). (D–F) Peak I-V plots of simulations using the same parameters of A–C, respectively. In each I-V plot, the experimental data are shown in black, and model predictions are shown in red. Fiber parameters: radius, 30 µm; length, 572 µm; capacitance, 4.9 µF/cm^2.